Hydrodynamic Thickness of Adsorbed Polymers in Steady Shear Flow

Yoram Cohen

Department of Chemical Engineering, University of California, Los Angeles, Los Angeles, California 90024. *Received November 24, 1986*

ABSTRACT: The effective hydrodynamic thickness (EHT) of adsorbed polystyrene in toluene and cyclohexane and poly(acrylamide) in aqueous NaCl solvent, both at the adsorption plateau, was determined in a steady laminar shear flow in an array of fused glass capillaries. Effective hydrodynamic thicknesses were determined for a shear rate range of 170–8000 s^{-1}, with an EHT resolution of about ±50 Å. The EHT for polystyrene in toluene, and for poly(acrylamide) in a 1200 ppm aqueous NaCl solvent, was found to decrease from the zero shear EHT values with increasing shear rate. The zero shear limit of the EHT in a Θ solvent (cyclohexane at 34.8 °C) was found to be lower than in a good solvent (toluene). In the Θ solvent, shear-thickening behavior of the adsorbed polymer layer was observed below a critical shear rate of about 4400 s^{-1}. Above the critical shear rate the EHT decreased with increasing shear rate. It is suggested that, below the critical shear rate, shear-induced disentanglement of subloops and/or the detachment of weakly anchored trains in the Θ solvent may be responsible for the rise in EHT.

1. Introduction

Polymer adsorption is of interest in numerous applications such as viscometry, liquid chromatography, wastewater treatment, microbial adhesion, ultrafiltration, and enhanced oil recovery. Much work has been done in order to quantify static adsorption isotherms and adsorbed polymer conformation as a function of the solvent power and polymer molecular weight. In recent years, there has been a growing interest in the interaction of fluid flow with adsorbed polymers.[1-13] Experimental studies have demonstrated that the average thickness of adsorbed polymer layers is a function of the wall shear rate.[2,3,7,12]

Different techniques are now available for measuring the average adsorbed layer thickness, such as photon correlation spectroscopy,[14] small-angle neutron scattering,[15,16] force-distance measurements between adsorbed polymer layers,[17] ellipsometry,[6,18] sedimentation,[19] and the hydrodynamic flow technique.[20-22] To date, however, only the hydrodynamic flow method and the ellipsometric technique have been employed to study the flow-induced deformation of adsorbed polymers.[2,7,8,12,13]

The hydrodynamic flow technique has been employed in flow through porous media,[12,20,21,23] capillary tubes,[3,9-11,24] millipore filters,[2,5,23,25] and porous membranes. In the hydrodynamic flow technique, the flow reduction due to adsorbed polymer is quantified in terms of an effective reduction in the diameter of the flow conduit expressed as an effective hydrodynamic thickness (EHT) of the adsorbed polymer layer. The early hydrodynamic flow studies were carried out at low shear rates and hence did not reveal a shear rate dependence of the EHT. The study of Thomas,[26] with a poly(acrylamide)–aqueous NaCl system, provided the first careful evidence, in a well-defined geometry, that the EHT decreases with shear rate. Recent studies have also demonstrated that the EHT varies with shear rate.[2,3,12,27]

Gramain and Myard[2] reported on the effect of solvent shear rate on the EHT for the flow of Newtonian solvents through millipore filters. They found that for both poly(acrylamide)–NaCl(aq) and polystyrene–toluene systems, the EHT values of the adsorbed polymer layer increased with increasing shear rate. Gramain and Myrad[2] reasoned that both shear and extensional flows could exist due to solvent flow through the adsorbed polymer layer; hence, the extensional component of the flow can lead to an increase in the EHT with increasing flow. The recent study of Idol and Andersen,[13] with poly(acrylic acid) (M_w = 150000) and polystyrenesulfonate (M_w = 690000) adsorbed from aqueous solutions in muscovite mica membranes demonstrated that the EHT may increase with increasing solvent flow rate only in pores less than 800 Å in diameter. In contrast, the study of Cohen and Metzner[2] with polystyrene–toluene, polystyrene–*trans*-Decalin, and poly(acrylamide)–water systems has shown that the EHT, measured in the flow of polymer solutions past adsorbed polymer layers, decreases with increasing shear rate. The above results demonstrated that, for good solvents, there is a steep initial decrease in the EHT at low shear rates and an asymptotic approach to a constant value of the EHT at high shear rates. The study of Cohen and Metzner,[3] however, is different from previous studies in that the measured EHT may have been affected by interactions of flowing polymer molecules with adsorbed macromolecules. A similar result for the EHT was obtained by Cohen and Christ[12] for the flow of 1250 ppm polyacrylamide in an aqueous 2% NaCl solution through silica packed beds.

The first study in which ellipsometry was utilized to investigate the shear rate dependence of an adsorbed polymer thickness was reported by Lee and Fuller[7] for a polystyrene–Θ solvent system (cyclohexane at 34.8 °C) in a slit geometry. A measurable change in the adsorbed layer thickness, over a shear rate range of zero to 7800 s^{-1}, was not observed for molecular weights of 1.8×10^6 and below. The adsorbed layer thickness for a 20 million molecular weight polystyrene was found to decrease from its zero shear thickness of 0.26 μm by about 15% as the velocity gradient increased to 8000 s^{-1}. In a companion study, with a cyclohexane–polystyrene system, Fuller and Lee[6] concluded that, at sufficiently high shear rates and shearing times, adsorbed polymer molecules may become detached from the surface by shear-induced desorption.

Several recent experimental studies have shown that the thickness of adsorbed polymer layers, measured by either ellipsometry or the hydrodynamic flow technique, increases with increasing solvent power even though the adsorbance (at the plateau region) decreases with increasing solvent power.[23-25,28-30] The findings of these studies suggest that the conformational change of adsorbed polymers, to a more collapsed form due to reduction in solvent power, may have a stronger effect on the EHT than the amount of adsorbed polymer. The above observation is contradicted by the recent theoretical analysis of Stuart et al.[31] which suggests that the EHT may decrease with increasing solvent power. Also worth noting is the study of Gramain and Myard,[23] who observed a decrease in the EHT of poly(acrylamide)

0024-9297/88/2221-0494$01.50/0

Table I
Polymer Characteristics and EHT at the Zero Shear Rate Limit

polymer	$10^6 M_w$	$\bar{M}_w/\bar{M}_n$	solvent	temp, °C	adsorbance, g/m²	L_{H_0}, μm	$2R_g$,[b] μm	t_{rms},[c] μm
poly(acrylamide)	5.5	1.23	1200 ppm NaCl(aq)	25	2×10^{-4}	0.34	0.31 (40)	
polystyrene	20	1.2	toluene	25	8.2×10^{-4}	0.45	0.55 (41)	0.35 (39)
polystyrene	20	1.2	cyclohexane	34.8[a]	6.54×10^{-3}	0.125	0.25 (41)	0.26 (7)

[a] Θ temperature for cyclohexane. [b] The numbers in parentheses correspond to the reference number. [c] t_{rms} is for a chrome plate surface.

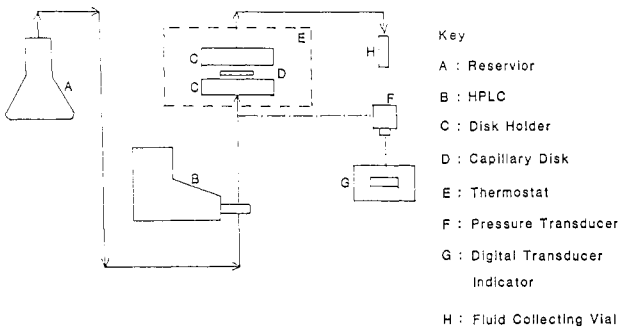

Figure 1. Schematic diagram of the experimental arrangement.

with increasing temperature above the Θ temperature (equivalent to increasing solvent power), a trend which is opposite to that observed by Kawaguchi and Takahashi,[30] above the Θ temperature, for the ellipsometric thickness of polystyrene in cyclohexane. An increase in the EHT with solvent power was also reported by Dejardin,[32] who demonstrated that the EHT for polystyrene in *trans*-Decalin, below the Θ temperature, increases as the Θ temperature is approached.

The differences in the fluids and surface geometries employed in past studies make it difficult to evaluate the coupled dependence of the EHT on solvent power and shear rate in simple shear flow. Thus, the purpose of this paper is to present an experimental investigation of the effect of shear rate on the EHT of adsorbed polymers in both a good and a Θ solvent in a well-characterized geometry.

2. Experimental Section

The shear rate dependence of the effective hydrodynamic thickness of polystyrene and poly(acrylamide) was studied in a specially designed capillary-disk rheometer. A schematic diagram of the experimental setup is shown in Figure 1. The experimental method of determining the EHT was based on the determination of the pressure drop–flow rate relationship for a given capillary disk in the presence and absence of adsorption effects.

2.1. Materials. The polymers used in this study were polystyrene (Pressure Chemical Co.) and partially hydrolyzed poly(acrylamide) (J333 mobility control polymer, 19% degree of hydrolysis, Dowell division of Dow Chemical USA). The poly(acrylamide) was fractionated by the method described by Francois et al.,[33] and its molecular weight was determined by GPC and intrinsic viscosity measurements.[33] The characteristics of the polymers used in this study are given in Table I. The solvents used for polystyrene were reagent grade cyclohexane and toluene. For poly(acrylamide), a 1200-ppm aqueous NaCl solution was used as a solvent. A millipore filter of a 0.8-μm pore size was used to filter the toluene and cyclohexane solutions of polystyrene and a 5-μm Nucleopore filters (Nucleopore Corp.) was used to filter the poly(acrylamide)–NaCl(aq) solution. All the solvents were filtered and degassed prior to the flow experiments.

2.2. Apparatus. The capillary-disk rheometer consisted of three major components: (i) a capillary disk mounted in a holder and immersed in a constant temperature water bath, (ii) a solvent delivery system, and (iii) a pressure-drop measuring system.

The capillary disk that consisted of a fused array of glass capillaries of uniform diameter was obtained from Galileo Electro-Optics Corp. (Sturbridge, MA). The geometrical properties of the disks are given in Table II. The average radius of the capillary tubes in each disk was determined from optical measurements by using a scanning electron microscope. The porosity was determined from knowledge of the number of capillary tubes per unit surface area and the average cross-sectional area of the tubes in each disk-type. Due to the small capillary diameter (2 and 5 μm), the effect of a polymer layer adsorbed onto the capillary wall is magnified relative to similar experiments with larger diameter tubes. Also, due to the large length to radius ratios of the disks, 200 and 500 for the 5- and 2-μm disks, respectively, end effects could be neglected without introducing any significant errors.

Table II
Geometrical Properties of Capillary Disks

disk no.[a]	av tube diameter, μm	no. of tubes/cm²	porosity
II	2.15	14.63×10^6	0.53
V	5.57	2.74×10^6	0.67

[a] Disk dimensions: 1 mm thick × 25 mm diameter.

The capillary disk was mounted in a disk holder made of stainless steel and constructed to hold interchangeable capillary disks. It consisted of two cylindrical sections each grooved and fitted with O-rings that sealed a portion of the capillary disk area perpendicular to the flow path. The actual flow area was determined from flow calibration experiments. Nitrile O-rings were used for cyclohexane and NaCl aqueous solutions while Viton O-rings were used for toluene. The disk holder was connected at one end to the solvent delivery pump through a swagelock fitting, with the effluent side feeding back to the solvent reservoir. Constant flow rate through the capillary disk was maintained by a microprocessor controlled high-pressure liquid chromatograph (Varian, Model 5000, Varian Associates) that allowed flow control with a maximum error of ±0.25% of the set flow rate. The experimental flow rates in the present work ranged from 0.09 to 1.3 mL/min. The solvent delivered to the capillary disk was continuously filtered by a built-in sintered stainless-steel filter with 2-μm pore size. The pressure drop across the capillary disk was monitored by a differential pressure transducer (Validyne Model DP15) with interchangeable diaphragms coupled with a digital transducer indicator (Validyne, Model CD23). Prior to each experiment, the pressure transducers were calibrated by using water or mercury U-tube manometers. The estimated error in the pressure drop measurements was no higher than 5%. Temperature control to within ±0.1 °C was achieved by immersing the entire disk holder assembly in a constant temperature bath and by controlling the solvent temperature through the HPLC unit.

2.3. Polymer Adsorption. Polymer adsorption onto the capillary walls was carried out after the preadsorption flow experiments without dismantling the disk holder. This procedure assured that the same flow area was used in both the preadsorption and postadsorption flow experiments. A freshly prepared polymer solution was first pumped through the capillary disk for a period of about 10 min. The outlet from the disk holder was plugged and the assembly was charged with the polymer solution. The top of the cell was plugged and the adsorption step was carried out in a temperature bath at the temperature of the flow experiments. The polymer solution was pumped periodically (about every 10 h) through the capillary disk in order to eliminate axial concentration gradients and thus assure a uniform surface coverage. An adsorption equilibration time of 1 week was determined to be sufficient to ensure that adsorption equilibrium has been reached.

The EHT dependence on shear rate was studied in the plateau region of the adsorption isotherms. Adsorption of polystyrene was carried out from a 1000 and 3000 ppm polystyrene solutions in toluene and cyclohexane, respectively. Adsorption from a

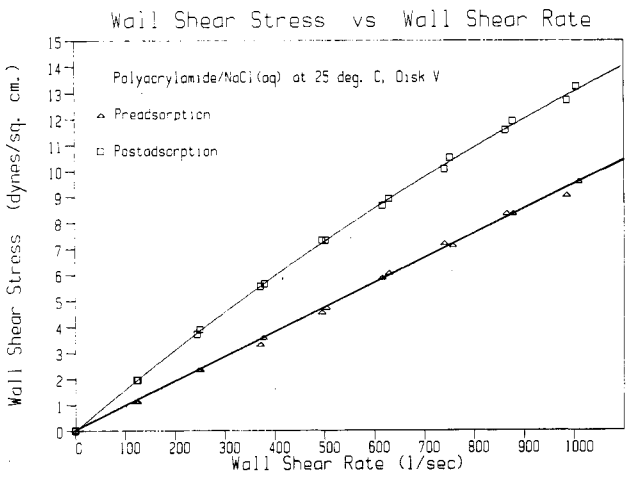

Figure 2. Effect of adsorbed poly(acrylamide) on the flow curves for a 1200-ppm aqueous NaCl solution (25 °C).

cyclohexane solution was carried out at the Θ temperature of 34.8 °C, and adsorption from toluene solution was carried out at 25 °C. Finally, adsorption of poly(acrylamide) was carried out at 25 °C from a 500 ppm polyacrylamide solution containing 1200 ppm NaCl. The above concentration of polystyrene and poly(acrylamide) are all higher than those required to reach the plateau region of the absorption isotherms.[12,23,34-39] The amounts of adsorbed polymer were determined from separate batch adsorption experiments.[12,35] The amounts adsorbed at the plateau region are given in Table I.

2.4. Postadsorption Flow Experiments. After the adsorption step, the disk holder with the capillary disk was mounted in the flow loop. A moderate flow rate of about 5 mL/min was first used to flush out any remaining nonadsorbed macromolecules from the flow channels. Flushing was continued for about 30 min after the HPLC's UV detector indicated a clear solution. The flow experiments were then initiated, and measurements were taken at successively higher flow rates. After the highest flow rate was reached, the identical measurement points were repeated at successively lower flow rates in order to check the reproducibility of the measurements. Reproducibility was found to be better than 99.5% for the flow rate range of 0.1–1.2 mL/min. Thus, it may be concluded that in our experiments any effects of polymer desorption were negligible.

The flow behavior in the presence and absence of the adsorbed polymer was expressed in terms of shear stress–shear rate plots.[3] The excess flow reduction due to adsorbed polymer layer was expressed as the effective hydrodynamic thickness, L_H, of the adsorbed polymer, given by

$$L_H/R = 1 - (\dot{\gamma}_a/\dot{\gamma})^{1/4} \quad (1)$$

where $\dot{\gamma}_a$ and $\dot{\gamma}$ are the apparent Newtonian shear rates in a single capillary (based on the actual capillary diameter), at a given wall shear stress level, in the absence and presence of polymer adsorption, respectively, and R is the capillary radius. We note that the ratio $\dot{\gamma}_a/\dot{\gamma}$ for a single capillary is equal to the ratio Q_a/Q, in which Q_a and Q are the flow rates through the entire array of capillaries in the flow area. The effective hydrodynamic thickness, L_H, was correlated with the wall shear rate, corrected for the effective reduction in the tube radius as suggested by Gramain and Myard.[2] Accordingly, the wall shear rate, corrected for the presence of the adsorbed polymer layer, is determined from

$$\dot{\gamma}_c = 4Q_a/\pi(R - L_H)^3 \quad (2)$$

3. Results and Discussion

The flow curves for the flow of toluene (at 25 °C), cyclohexane (at the Θ temperature), and the 1200 ppm aqueous NaCl solution through the capillary disks with and without an adsorbed polymer layer are shown in Figures 2–4. Each flow curve was obtained from multiple runs carried out on different days. The average deviation between runs was less than ca. 2%. The preadsorption data

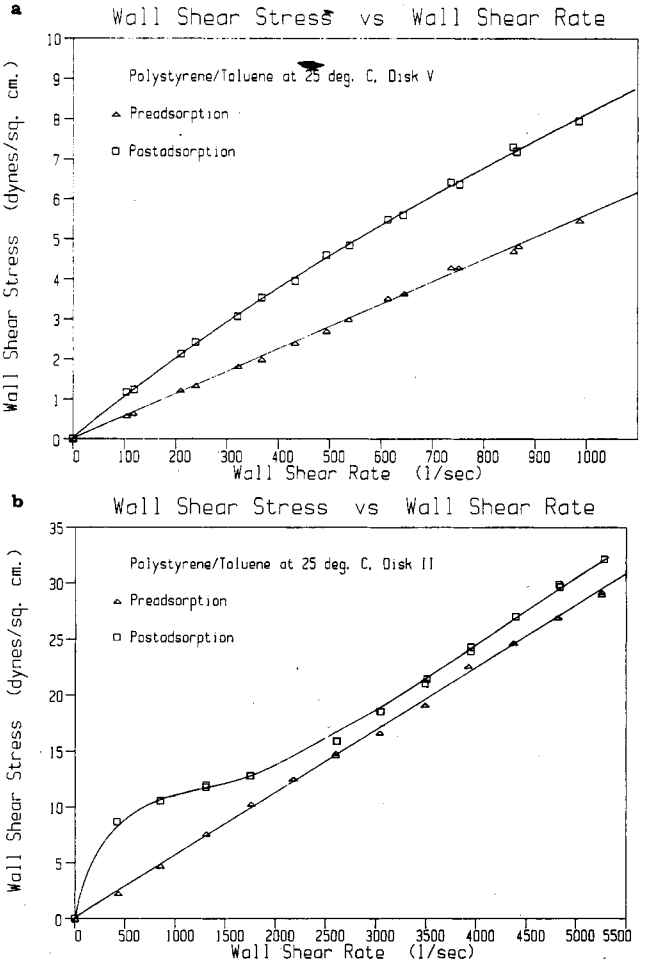

Figure 3. (a) Effect of adsorbed polystyrene on the flow curves for toluene (25 °C). (b) Effect of adsorbed polystyrene on the flow curves for toluene (25 °C) at high shear rates.

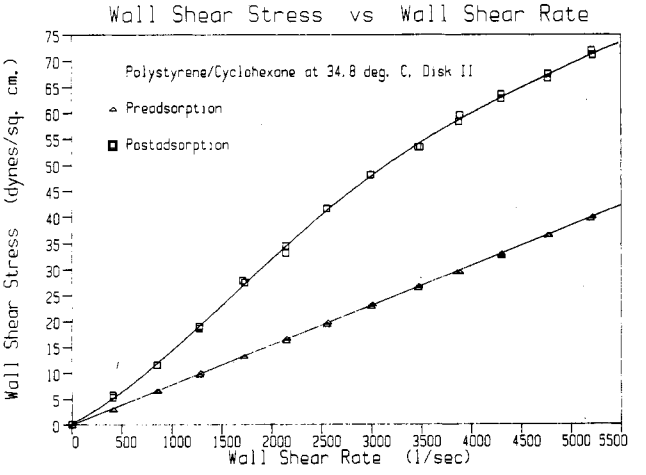

Figure 4. Effect of adsorbed polystyrene on the flow curve for cyclohexane (at 34.8 °C).

followed straight lines, with correlation coefficients no smaller than 0.998, as expected for a fully developed Poiseuille flow. The separation of the pre-adsorption and postadsorption flow curves, at a given capillary wall shear stress (τ_w), indicates that there is significant flow reduction due to the adsorbed polymer layer. Furthermore, the nonlinear shear stress–shear rate behavior for the postadsorption experiments (Figures 2–4) suggests that the thickness of the adsorbed layer is a function of the wall shear rate. The effective hydrodynamic thickness, L_H, was determined from eq 1, and the resulting corrected shear

rate (eq 2) dependence of L_H is shown in Figures 5 through 7.

3.1. EHT in the Limit of Zero Shear Rate. Most of the early studies which utilize the hydrodynamic flow method of studying the EHT of adsorbed polymers were done at shear rates well below 10 s^{-1}. Therefore, the EHT reported in these studies is more closely associated with the zero shear limit of the EHT, L_{H_0}. Although the lowest corrected wall shear rate (eq 2) in this work was 170 s^{-1}, it is instructive to compare the extrapolated L_H at the zero shear limit to both the root-mean-square thickness, t_{rms}, obtained from ellipsometric measurements of adsorbed polymers and the radius of gyration, R_g, of the free polymer in solution (Table I).

It has generally been accepted in previous studies that in a Θ solvent $L_{H_0} \approx 2R_g$[20,21,40] while L_{H_0} can be much greater than $2R_g$ for high molecular weight polymers in good solvents.[2,23,31,34,40,41] The current results (Table I) indicate that $L_{H_0} \approx 2R_g$ for polyacrylamide in aqueous NaCl solution which is in agreement with previous studies.[23,26] Additionally, our results demonstrate that L_{H_0} for polystyrene in the Θ solvent is smaller than in a good solvent, as expected, since the contribution of dangling tails to L_{H_0} increases.[31] The results for polystyrene, however, in either a Θ or good solvent reveal that $L_{H_0} < 2R_g$. The data of Gramain and Myard[2] for polystyrene–toluene system indicate that $L_{H_0} < 2R_g$ for $M_w > 2.4 \times 10^6$, in partial support of our results. It is also interesting to note that the extrapolated data of Kawaguchi et al.[39] for polystyrene of $M_w = 2 \times 10^7$ adsorbed onto a chrome plate reveals that the t_{rms} in toluene is smaller than $2R_g$. The recent study of Kawaguchi et al.[25] has also shown that the L_{H_0} for narrow molecular weight fractions of poly(ethylene oxide) ($M_w = 4 \times 10^4$ to 1.2×10^6), adsorbed in cellulose ester Millipore filters, is much smaller than $2R_g$. Similar behavior was reported by Cosgrove et al.,[16] who observed that the EHT, obtained from photon correlation spectroscopy, for PEO adsorbed onto polystyrene latex particles, was less than $2R_g$ for molecular weights of less than about 6.6×10^5 but exceeded the value of $2R_g$ by less than about 4.1% at higher molecular weights. We also note that adsorption capacity for polystyrene ($M_w = 2 \times 10^7$) adsorbed on glass, from cyclohexane, is approximately 6.54×10^{-3} g/m^2 compared with a value of 5.2×10^{-3} g/m^2 for a chrome plate Takahashi et al.[36] The adsorbance (at the plateau region) from toluene (35 °C) onto a chrome plate is 6.5×10^{-4} g/m^2 [39] compared to an adsorption capacity of 8.2×10^{-4} g/m^2 for polystyrene adsorbed from toluene onto a silica surface. The higher adsorption capacity of polystyrene on glass, and the fact that in our study $L_{H_0} < 2R_g$ for both the Θ and good solvent conditions, suggests that polystyrene adsorbs strongly in the glass capillaries which results in a more flattened configuration. This assertion is consistent with Kawaguchi et al.,[25] who reasoned that the strong adsorption of poly(ethylene oxide) in cellulose ester millipore filters compared to the weaker adsorption on polystyrene lattices may result in a flatter conformation on the cellulose ester substrate.

3.2. Variation of EHT with Wall Shear Rate. The dependence of the EHT on shear rate for adsorbed polyacrylamide for the flow of a 1200 ppm NaCl aqueous solution is shown in Figure 5. The dependence of the EHT on shear rate for polystyrene in a good solvent (toluene at 25 °C) and in a Θ solvent (cyclohexane at 34.8 °C) are shown in Figures 6 and 7.

The EHT for poly(acrylamide) decreased with increasing shear rate which is in qualitative agreement with the findings of Cohen and Metzner,[3] Cohen,[27] and Cohen and Christ.[12] As shown in Figure 5 the shear rate dependence of L_H determined from the data of Thomas,[26] who also used an array of fused glass capillaries in his study with polyacrylamide ($M_w = 5.5 \times 10^6$), is in good agreement with the current study. The differences are attributed the fact that Thomas[26] adsorbed polyacrylamide from a flowing 250 ppm solution compared with static adsorption from a 500 ppm solution used in the current study. Consequently, one might expect a lower adsorption coverage for the Thomas

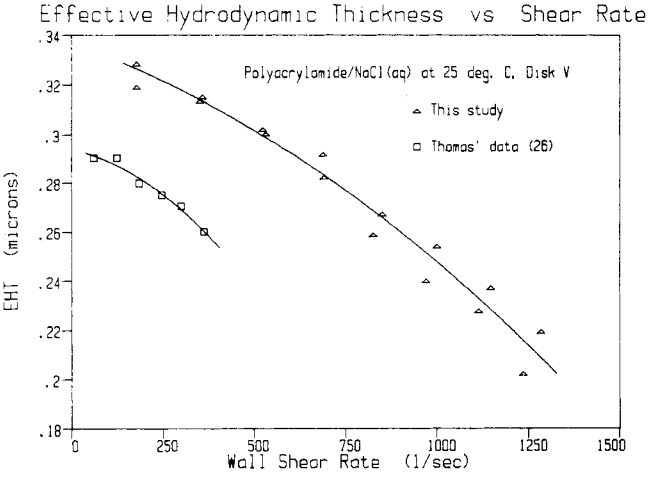

Figure 5. Dependence of effective hydrodynamic thickness on corrected shear rate ($\dot{\gamma}_c$) for adsorbed poly(acrylamide) in 1200-ppm NaCl solution.

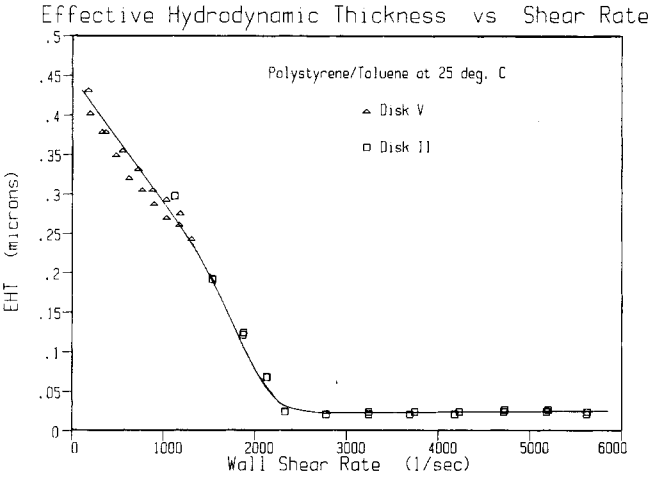

Figure 6. Dependence of effective hydrodynamic thickness on corrected shear rate ($\dot{\gamma}_c$) for adsorbed polystyrene in toluene.

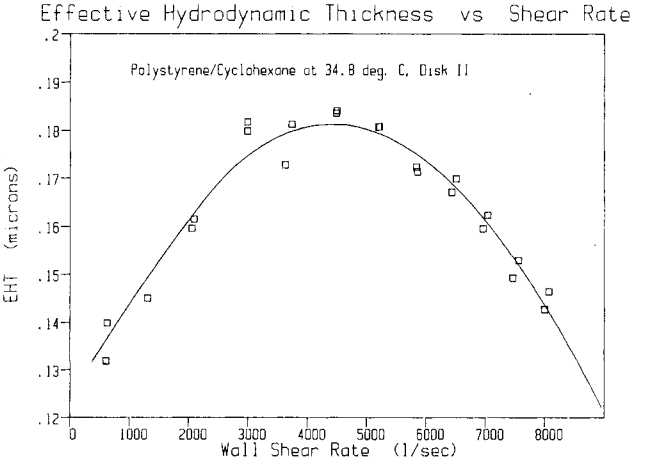

Figure 7. Dependence of effective hydrodynamic thickness on corrected shear rate ($\dot{\gamma}_c$) for adsorbed polystyrene in cyclohexane.

study. In contrast with the above shear rate dependence, Gramain and Myard[2] found that the EHT for poly(acrylamide) (in 0.3–0.5 M aqueous NaCl solution) increased with increasing shear rate, in nucleopore filters of pore diameter 0.3–0.8 μm. The results of the studies of Gramain and Myard[2] and Idol and Andersen[13] suggest that there may be a critical ratio of the radius of gyration to pore radius above which shear thickening behavior can occur. More work, however, is needed in order to explore this hypothesis.

The EHT for polystyrene in a good solvent (toluene) was found to decrease with increasing shear rate toward an asymptotic (limiting) value of about 0.02 μm (Figure 7). This behavior is in qualitative agreement with the observation of Cohen and Metzner[3] for the EHT of polystyrene subjected to the flow of a 4% polystyrene solution in toluene. The EHT dependence on shear rate can be reasoned on the basis of the models of Lee and Fuller[7] and Hatano[8] for an adsorbed dumbbell molecule. When anchored loops and tails which protrude from the surface are subjected to a shear flow, the exerted drag force will tend to carry the loops and tails along the flow direction. Simultaneously, the Brownian motion force and the spring force of the polymeric chain will act to balance the drag force. As the drag force increases with increasing solvent velocity, loops and tails will lean over to a new position closer to the surface where the solvent velocity and thus the drag force are smaller. Therefore, a force balance can be attained at that new position. As the shear rate increases, the location at which the force balance can be maintained becomes closer to the surface. It is worth noting that the decrease in the thickness of the adsorbed dumbbell molecule is only predicted for a nonlinear spring force.[4,7] For the polystyrene–toluene system, at sufficiently high shear rates (above about 2500 s^{-1}) the loops and tails are brought to a position, just above the surface, where the monomers are closely compacted. At this latter condition further decrease in the layer thickness is no longer possible and the EHT reaches its limiting value (Figure 7).

In contrast with the above results, the EHT in a Θ solvent (cyclohexane at 34.8 °C) was observed to increase with shear rate up to a maximum value (about a shear rate of 4400 s^{-1}) and then decrease as the shear rate continued to increase. Although the shear-thickening behavior of adsorbed polymer layers has been previously observed,[2,13] the transition from shear-thickening to shear-thinning behavior of the EHT is reported here for the first time. The dependence of the EHT of polystyrene on shear rate in a Θ solvent is closely linked to the density of surface coverage by adsorbed polymer. The studies of Linden and Leemput[35] and Takahashi et al.[36] suggest that nearly all the active sites on silicious surfaces are occupied by polystyrene segments. Consequently, the surface of the capillary walls is densely covered with adsorbed polystyrene molecules. On a surface with densely populated polymer molecules, steric hinderance is important. Therefore, below a critical shear rates the drag force may be too small to overcome these steric effects and to drag the tails and loops closer to the surface. At the Θ condition segmental interactions are negligible, and hence in a density covered surface it is possible for subloops, weakly adsorbed trains, and collapsed tails to exist. This hypothesis is consistent with the study of Furusawa and Yamamoto,[37,38] who concluded that in the case of polystyrene adsorption from cyclohexane (at the Θ temperature) onto silica about 25% of the adsorbed molecules are weakly adsorbed. Thus, below the critical shear rate, as the shear rate is increased, loops and trains that are anchored by floating trains (those whose attractive forces might be weak) may be separated from the surface. Consequently, below the critical shear rate, the EHT rises with increasing shear rate. The above hypothesis is supported by the model of Hatano[8] for an adsorbed dumbbell molecule. These authors have suggested, based on their theoretical model of an adsorbed dumbbell molecule, that a critical shear rate exist below which shear-thickening behavior of adsorbed polymer layers is possible. Above the critical shear rate the EHT decreases with increasing shear rate. It is noted that the values of the EHT for cyclohexane, at a given shear rate level, are higher than for toluene. This behavior can be attributed to the higher surface density and hence steric hinderance that lowers the degree of adsorbed polymer deformation at a given shear rate. Finally, it is emphasized that this shear thickening behavior is particularly apparent through EHT measurements due to the sensitivity of the hydrodynamic method to the presence of tails.

4. Conclusions

This study has shown that the EHT of an adsorbed polymer layer, in a good solvent, decreases with shear rate to a constant limiting value that is reached at a sufficiently high shear rate. In a Θ solvent, below a critical shear rate, the EHT increases with increasing shear rate and it decreases with shear rate above the critical shear rate. Below the critical shear rate, as the shear rate increases, the disentanglement of internal subloops or tails or the detachment of weakly adsorbed trains are believed to be responsible for the initial increase in the EHT for Θ solvents.

Acknowledgment. This work was supported in part by the National Science Foundation Grant CBT-8416719, the University of California, Water Resources Center Project UCAL-WRC-W-660, the U.S. Geological Survey, Department of the Interior, under award 14-08-0001-G-1315, and the University of California Toxic Substance Research and Teaching Program. The author also acknowledges Mr. Chih-Hao Tsang and Mr. Varun Taepaisitphongsi who contributed to this work.

Registry No. Polystyrene, 9003-53-6; poly(acrylamide), 9003-05-8; toluene, 108-88-3; cyclohexane, 110-82-7; sodium chloride, 7647-14-5.

References and Notes

(1) Dimarzio, E. A.; Rubin, R. J. *J. Polym. Sci., Polym. Phys. Ed.* **1978**, *16*, 457.
(2) Gramain, Ph.; Myard Ph. *Macromolecules* **1981**, *14*, 180.
(3) Cohen, Y.; Metzner, A. B. *Macromolecules* **1982**, *15*, 1425.
(4) Fuller, G. F. *J. Polym. Sci., Polym. Phys. Ed.* **1983**, *21*, 151.
(5) Chauveteau, G.; Tirrell, M.; Omari, A. *J. Colloid Interface Sci.* **1984**, *100*, 41.
(6) Fuller, G. G.; Lee, J.-J. In *Polymer Adsorption and Dispersion Stability*; Goddard, E. D., Vincent, B., Eds.; ACS Symposium Series 240; American Chemical Society: Washington, DC, 1984.
(7) Lee, J.-J.; Fuller, G. G. *Macromolecules* **1984**, *17*, 375.
(8) Hatano, A. *Polymer* **1984**, *25*, 1198.
(9) Hikmet, R. A. M.; Narh, K. A.; Barham, P. J.; Keller, A. *Prog. Colloid Polym. Sci.* **1985**, *71*, 32.
(10) Barham, P. J.; Hikmet, R. A. M.; Narh, K. A.; Keller, A. *Colloid Polym. Sci.* **1986**, *264*, 515.
(11) Narh, K. A.; Barham, P. J.; Hikmet, R. A. M.; Keller, A. *Colloid Polym. Sci.* **1986**, *264*, 507.
(12) Cohen, Y.; Christ, F. R. *SPE Reservoir. Eng.* **1986**, 113.
(13) Idol, W. K.; Andersen, J. L. *J. Membrane Sci.* **1986**, *28*, 269.
(14) Garvey, M. J.; Tadros, Th. F.; Vincent, B. *J. Colloid Interface Sci.* **1976**, *55*, 440.
(15) Barnett, K. G.; Cosgrove, T.; Vincent, B.; Burgess, A. N.; Crowley, T. L.; King, T.; Turner, J. D.; Tadros, Th. F. *Polymer* **1981**, *22*, 283.
(16) Cosgrove, T.; Crowley, T. L.; Stuart Cohen, M. A. In *Polymer Adsorption and Dispersion Stability*; Goddard, E. D., Vincent,

B., Eds.; ACS Symposium Series 000; American Chemical Society: Washington, DC, 1984.
(17) Luckham, P. F.; Klein, J. *Nature (London)* **1983**, *300*, 429.
(18) Stromberg, R. R.; Thutas, D. J.; Passaglia, E. *J. Phys. Chem.* **1965**, *69*, 3995.
(19) Fontana, B. J.; Thomas, J. R. *J. Chem. Phys.* **1961**, *65*, 480.
(20) Rowland, F. W.; Eirich, F. R. *J. Polym. Sci., Polym. Chem. Ed.* **1966**, *4*, 2401.
(21) Rowland, F. W.; Eirich, F. R. *J. Polym. Sci., Polym. Chem. Ed.* **1966**, *4*, 2033.
(22) Kniewske, R.; Kulicke, W. M. *Makromol. Chem.* **1983**, *184*, 2173.
(23) Gramain, Ph.; Myard, Ph. *J. Colloid Interface Sci.* **1981**, *84*, 114.
(24) Varoqui, R.; Dejardin, Ph.; Pefferkorn, E. In *Adsorption at the Gas-Solid and Liquid-Solid Interface*; Rouquerol, J., Sing, K. S. W., Eds.; Elsevier: Amsterdam, 1982.
(25) Kawaguchi, M.; Mikura, M.; Takahashi, A. *Macromolecules* **1984**, *17*, 2063.
(26) Thomas, C. P. *Soc. Pet. Eng. J.* **1976**, 130–136.
(27) Cohen, Y. In *Advances in Rheology*; Mena, B., Garcia-Rejon, A., Rangel-Nafaile, C., Eds.; Universidad National Autonoma De Mexico, 1984; Vol. 2, p 299.
(28) Pefferkorn, E.; Dejardin, P.; Varoqui, R. *J. Colloid Interface Sci.* **1978**, *63*, 353.
(29) Kawaguchi, M.; Takahashi, A. *J. Polym. Sci., Polym. Phys. Ed.* **1980**, *18*, 2069.
(30) Kawaguchi, M.; Takahashi, A. *Macromolecules* **1983**, *16*, 1465.
(31) Stuart Cohen, M. A.; Waajen, F. H. W. H.; Cosgrove, T.; Vincent, B.; Crowley, T. L. *Macromolecules* **1984**, *17*, 1825.
(32) Dejardin, Ph. *J. Phys.* **1983**, *44*, 537.
(33) Francois, J.; Sarazin, D.; Schwartz, T.; Weill, G. *Polymer* **1979**, *20*, 969.
(34) Silberberg, A. *Colloques Internationaux du CNRS*; Polymers E.T. Lubrication Brest, France, May 1974, No. 233.
(35) Linden, C. V.; Van Leemput, R. *J. Colloid Interface Sci.* **1978**, *67*, 48.
(36) Takahashi, A.; Kawaguchi, M.; Hirota, H.; Kato, T. *Macromolecules* **1980**, *13*, 884.
(37) Furusawa, K.; Yamamoto, K. *J. Colloid Interface Sci.* **1983**, *96*, 268.
(38) Furusawa, K.; Yamamoto, K. *Bull. Chem. Soc. Jpn.* **1983**, *56*, 1958.
(39) Kawaguchi, M.; Hayakawa, K.; Takahashi, A. *Macromolecules* **1983**, *16*, 631.
(40) Varoqui, R.; Dejardin, P. J. *J. Chem. Phys.* **1977**, *66*, 4395 and references therein.
(41) Willhite, G. P.; Dominguez, J. G. In *Improved Oil Recovery by Surfactants and Polymer Flooding*; Shah, D. O., Schechter, R. S., Eds.; Academic: New York, 1977 and references therein.

Physical and Dynamic Mechanical Properties of Ultradrawn Polypropylene Films

S. K. Roy, T. Kyu,† and R. St. John Manley*

Pulp and Paper Research Institute of Canada and Department of Chemistry, McGill University, Montreal, Quebec, Canada H3A 2A7. *Received May 18, 1987*

ABSTRACT: Dynamic mechanical measurements were made on gel films of high molecular weight polypropylene prepared by gelation/crystallization from 1% (w/v) decalin solutions. The measurements were performed at different frequencies in the temperature range from −160 °C to the melting point of the sample. The dry gel films were uniaxially drawn at 150 °C to various draw ratios (λ) between 6.5 and 48. The morphology and orientation of the samples were characterized by density, differential scanning calorimetry, infrared dichroism, wide-angle X-ray diffraction, small-angle light scattering, scanning electron microscopy, and dynamic storage modulus. WAXS studies showed that very high degrees of orientation were achieved at the higher draw ratios. SEM of highly drawn specimens revealed that the initially random texture of crystallites transforms into fibrous form with the fiber axis parallel to the draw direction. DSC and density measurements show that the melting point and crystallinity increase with λ, reaching a maximum at λ = 30. The complex elastic modulus (E^*) increased with increasing λ and leveled off beyond λ = 40. In the dynamic mechanical measurements the γ peak was either weak or absent in both the loss tangent (tan δ) and loss modulus curves. At a given frequency, the β-relaxation intensity decreased and shifted to lower temperatures with increasing λ. Activation energies (ΔH) of the β dispersion process were obtained from an Arrhenius-type plot of log frequency versus the reciprocal temperature of the β-dispersion maximum. The values of ΔH ranged from 59 to 119 kcal/mol. In the crystalline α-relaxation region a sharp rise in tan δ was observed and the α-peak position shifts to higher temperature with increasing λ. The activation energy for this process is about 53 kcal/mol. On the basis of the dynamic mechanical measurements the origins of the various relaxation processes are discussed.

Introduction

The mechanical relaxation processes of polypropylene have been relatively less studied in comparison with numerous studies of polyethylene.[1] Isochronal dynamic mechanical properties of polypropylene over a wide temperature range were first investigated by Flocke.[2] These measurements were conducted with a torsion pendulum instrument operating at approximately 1 Hz. Three relaxation peaks, identified as α, β, and γ in descending order of temperature, were observed. The intermediate β peak around 0 °C was found to be very intense and was identified with the glass transition temperature. Passaglia and Martin attributed this peak to the atactic fraction of the polymer.[3] From dynamic X-ray and dynamic birefringence studies on melt-crystallized polypropylene, Kawai et al. concluded that the β-mechanical relaxation is an interlamellar grain boundary phenomenon.[4,5] The lowest temperature γ-relaxation in the vicinity of −100 °C is weak or absent and has been attributed to the local motions in the amorphous fraction of the polymer.[6,7] McCrum attributed the highest temperature α-relaxation to the crystalline morphology of polypropylene.[8] On the basis of dynamic X-ray diffraction studies of melt-crystallized spherulitic material, Kawai et al.[5] have recently suggested that the α process in polypropylene is of intralamellar origin, involving lamellar tilting in the polar zone of the spherulites.

* To whom correspondence should be addressed.
† Department of Polymer Engineering, College of Engineering, University of Akron, Akron, Ohio 44325.

0024-9297/88/2221-0499$01.50/0